Organic Solar Cells with colloidal PbS nanocrystals

Bachelor project
Hilbert Dijkstra

31-08-2009

rijksuniversiteit groningen

faculteit wiskunde en natuurwetenschappen

Abstract

This thesis reports about the research in the application of colloidal nanocrystals in organic solar cells. In order to make organic solar cells sensitive in the near infrared and in addition increase the efficiency of solar cells, PbS nanocrystals are added to the well known P3HT/PCBM blend. Thin films composed by the 3component blend, made by doctor-blading and spin-coating, are used as active layer of solar cells. Efficiencies slightly above the 2% are achieved, however limited reproducibility of the results is obtained. The control of the morphology of the active layer turned out to be very challenging.

1 Introduction

Nowadays, two of the world's biggest challenges to overcome are the climate crisis and the energy crisis.
Since the industrial revolution and the use of fossil fuels, the emission of carbon dioxide and other polluting materials, is increasing each year. As a result, the temperature close to the earth surface and oceans is increasing. This phenomenon is called global warming. The increase of the average temperature could cause several undesired environmental changes like the melting of the arctic ice, the rise of sea level throughout the world, and extreme weather conditions.

Moreover, the increased usage of fossil fuels is exhausting the world's fossil fuels stock.
To overcome both the climate crisis as well as the energy crisis, there is a urgent need for clean and renewable energy sources of which solar energy is an excellent example.

Solar energy is a promising candidate to fulfil this need for new energy sources. There are several technologies that allow to use the sun as source of energy, one of them is the photovoltaic cell (PVC). In the PVC's sunlight is directly converted into electricity thanks to the active layer composed by semiconducting materials. The energy of the incident photon, coming from sunlight, is $h\nu$, needs to be larger then the energy band gap between the conduction and valence band of the semiconductor. In this case the electron is excited from the valence band into the conduction band and a hole is left in the valence band. In order to achieve good solar cell performances, the created electron-hole pairs need to be separated and move to the cathode and anode, respectively.

Commercially available PVC's are generally based on silicon. They exhibiting high efficiency, but are very expensive and complex to produce. Alternative ways to decrease the cost and overcome the disadvantage of silicon based solar cells are at the moment under investigation. In the case of organic base solar cells the production process is much easier and potentially less expensive. Besides the easier production, the organic materials have high absorption coefficients, compared with Silicon, which means that the layers can be thinner. Another advantage is the flexibility of the organic solar cells which makes them more suitable for integration in buildings of high architectural value.

Most of the carbon-based materials are insulating, but conjugated organic materials such as conjugated polymers and oligomers are conductive. The discovery of the electronic property of conjugated carbon-based material has induced numerous applications in electronics and optoelectronics. One of these

applications is as active layer in solar cell. Recently, the most investigated PVC's are based on a blend of conjugated polymer and a fullerene derivative. The best examples nowadays reach 7.8% which was achieved by Solarmer and Heliatek, however the most investigated organic solar cell are based on P3HT/PCBM and exhibiting as record efficiency ~5% [1].

Silicon based solar cells have efficiencies in the range from ~10% - 25% [1]. The low efficiency and the limited lifetime are significant disadvantages of organic solar cells. When organic solar cells are exposed to air the efficiency significantly decreases. This is mainly due to oxygen and water, which act as charge traps damaging the solar cell performances.

P3HT has an absorption spectral range from around 400 nm to 600 nm [18]. Nowadays the most solar cells absorb in the visible spectral range but half of the sun's power reaching the earth's surface lies in the infrared. Therefore it is important to shift the absorption to the near infrared.

Here we report on attempts to increase the efficiency of organic solar cell by adding nanocrystals which absorb in the near infrared. By controlling the nanocrystals size during synthesis the optoelectronic properties can be tuned due to the quantum confinement which describes how the organization of the energy levels changes by size. On this way the bandgap of nanocrystals becomes tunable. The absorption edge of nanocrystals based on PbS can be tuned between 900 nm and 1500 nm, making of them good candidates for the near-infrared sensitization of organic solar cells.

In chapter two, the theory behind the organic solar cells and its characterization are discussed. Details about the experiments, materials and the processing are given in the third chapter. The results obtained are shown and discussed in chapter four. Conclusions that can be extracted from the research will be presented in the fifth chapter.

2 Theory

In the following chapter the working principles of an organic solar cell will be discussed with detailed characterization and determination of the most important parameters of the solar cells. Later on, solar cells based on P3HT/PCBM and photovoltaic devices, containing PbS, will be introduced.

2.1 Organic Solar Cells

The organic solar cell based on a photoactive layer, which is sandwiched between two electrodes. One of these electrodes needs to be transparent to let the light go through and reach the photoactive layer. In the photoactive layer excitons will be created by the incident light. An exciton consists of a bound state of an electron and a hole which needs to be separated and transferred to the respective electrodes to generate a current.

For the transport of the charge carriers two different materials are used; one which transfers the electrons and one which transfers the holes. For the transport of the hole, a hole conducting polymer is normally used.

Conjugated polymers have single and double bonds alternating with each other. A single bond consists of an σ-bond and the double bond consists of both an σ-bond and a Π-bond. The electrons in the Π-bond are mobile and because of the overlap of the orbitals along the conjugation path forms a Π-band in which it is possible for the electrons to 'jump' from site to site between the carbon atoms. The filled Π-orbital is called the HOMO (Highest Occupied Molecular Orbital) and the empty Π-orbital is called the LUMO (Lowest Unoccupied Molecular Orbital) [2]. The HOMO-LUMO gap is comparable but not identical to a band gap as is known in semiconductor physics. The typical HOMO-LUMO gap is roughly ranging from 1-4 eV for these kinds of materials.

When there is an exciton created in the photoactive layer the charge carriers need to be separated and transferred towards the electrodes. This is done by making the two electrodes, between which the photoactive layer is sandwiched, of different material. One of the electrodes is made of a material with a high work function and the other electrode with a low work function. Because of this difference in work function a built-in electron field appears between the electrodes. In this way the electrons will be extracted by the low work function electrode – which is the cathode - and the holes by the high work function electrode – which is the anode as in agreement with the definition of anode and cathode.

The system in which a blend of two materials is used to create charge carrier separation and in which each material transfers one of the charge carriers is called the donor/acceptor or type 2 heterojunction. The donor/acceptor couple consists of two materials with different electron affinities and ionization potentials. When an exciton is generated it diffuses to the D/A interface; the acceptor has a larger electron affinity and will therefore "accept" the electron. In the same way, the hole will be accepted by the donor resulting in charge separation. Once the charge carriers are separated at the D/A interface the hole can be transferred to the cathode and the electron can be transferred to the anode. Notice that the difference in potential energy needs to be larger than the exciton binding energy; otherwise charge separation can not occur [5].
A well known and widely used acceptor, in the planar heterojunction cell, is the buckyball C_{60} molecule, in which 60 electrons form a delocalized Π system which is similar to that in conjugated polymers. When C_{60} is used as acceptor in combination with a polymer donor, most of the light will be absorbed by the polymer [6]. When the exciton is created in the polymer it diffuses to the D/A interface where the electron is transferred from the LUMO of the donor to the LUMO of the acceptor. When the charges are separated, again both the electron and the hole can be transferred to the proper electrodes.

When such D/A layer are used instead of a single material layer there is a significant increase in power conversion efficiency of ~ 1% [6].
This increase is due to the charge separation, which is far more efficient in the D/A layer. The typical diffusion length of the exciton in conjugated polymers is about 5-7 nm [19], so only excitons generated near the D/A interface are able to reach the interface. Excitons that are further away (> 10 nm) won't reach the interface but recombine. This problem is solved by the bulk heterojunction approach. A bulk heterojunction consist of an interpenetrating network of a donor/acceptor mixture. In this way a high interfacial area is created and at each point in the composite there is a D/A interface on a few nanometers scale which allows for more excitons to reach the D/A interface [2].

2.2 Characterization of organic solar cells

Solar cells are generally characterized by measuring J-V characteristics in dark and under illumination in order to extract the most important parameters of the cells:

- the open circuit voltage, the voltage at which J=0
- the short circuit current, the current when there is no applied voltage
- the maximum power point, the point at which the area below the J-V curve is maximized

A J-V curve is plotted in figure 1 to clarify the parameters which are denoted above.

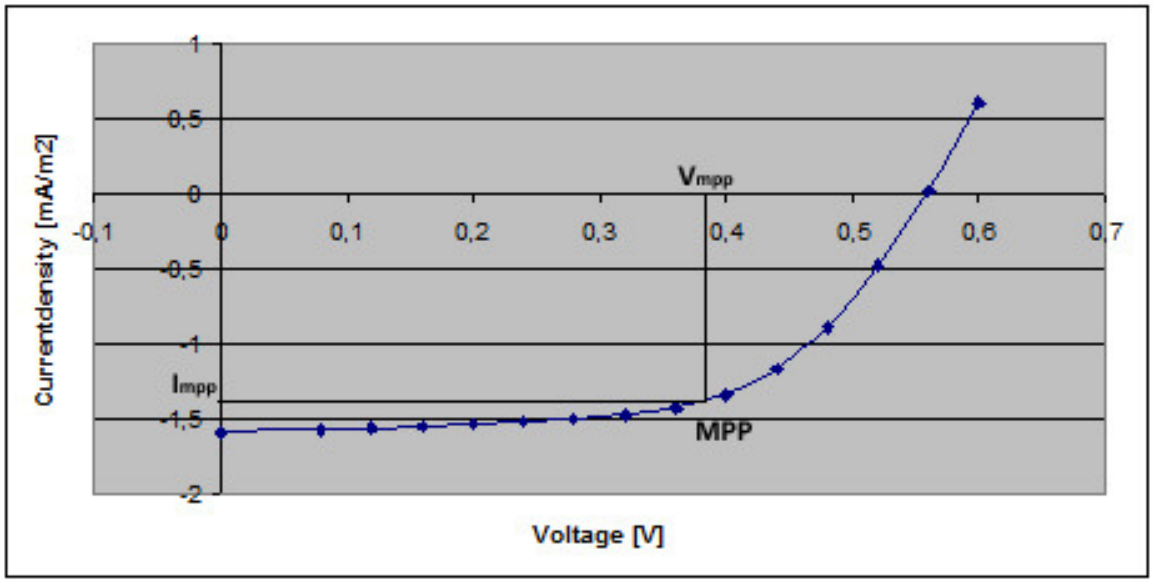

Fig. 1: Typical J-V curve of the organic solar cells.

Using these parameters the fill factor (FF) and the power conversion efficiency (η) can be extracted. The fill factor is the measure of the shape of the J-V curve and is defined as:

$$FF = \frac{J_{MPP} \times V_{MPP}}{J_{SC} \times V_{OC}} \qquad 2.1$$

This is the ratio between the maximum power and the product of J_{SC} and V_{OC}, which is, theoretically, the maximum power that the solar cell can deliver.
The power conversion efficiency can be calculated by using:

$$\eta = \frac{J_{SC} \times V_{OC} \times FF}{P_{IL}} \qquad 2.2$$

J_{SC}, V_{OC}, FF and η are the key performance parameters of the solar cell. All these parameters should be defined for particular illumination conditions. One of the standard illumination conditions is the Standard Test Conditions (STC) which includes constant temperature for the solar cell (25 °C), a light intensity of 1000 W/m^2 and a spectral distribution of the light of AM 1,5 which means that the solar light has been filtered by 1,5 km of earth's atmosphere. [2]
Another important feature of solar cells is the external quantum efficiency, called EQE, which describes the relation between the photocurrent density and the incident spectrum. The EQE is the ratio between the number of electrons per second extracted by the device and the number of photons per second incident on the solar cells. With the EQE gives the number of photons which are needed to

create one electron. The EQE is independent on the incident spectrum and is therefore a very useful key to describe the performance of the solar cell under different conditions from the STC. [2]

2.3 Solar cells based on P3HT/PCBM

A commonly used and investigated donor/acceptor couple consists of P3HT/PCBM couple. PCBM is a functionalized derivative of C_{60} molecule that at the opposite of the parent system is soluble in many organic solvents. The P3HT is a polymer composed by thiophenes units, it is an excellent hole conductor and can display electron donating properties in combination with PCBM. Recently, solar cells having a blend of P3HT and PCBM as active layer exhibit efficiencies up to 5% [7].
The HOMO and the LUMO of P3HT are at –4,9 eV and –3,0 eV and the HOMO and LUMO level of PCBM are –6,1 eV and –4,3 eV therefore the P3HT has an optical band gap around 1,9 eV and for PCBM the optical band is around 1,8 eV. The hole mobility of P3HT is ~0.1 cm^2/V s and the electron mobility of PCBM is $2*10^{-3}$ cm^2/V s [7, 11].
When the device is produced, the cell's efficiency can be further improved by annealing the device. Annealing causes re-crystallization, which has a positive effect on the hole mobility, but next to this it also reduces the free volume and the density of defects at the interface. In figure 2 the characteristics of a P3HT-PCBM cell are shown and how they vary when they are annealed at different temperatures [8].

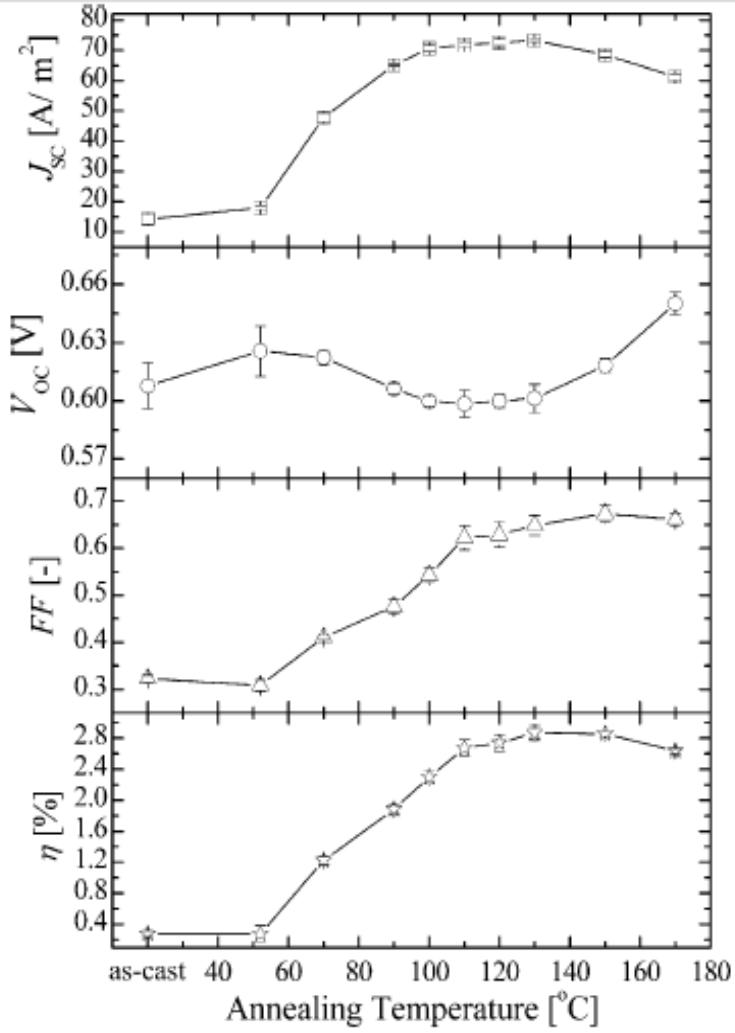

Fig. 2: The behaviour of J_{SC}, V_{OC}, FF and the η when a 50-50 wt.-% P3HT-PCBM blend was annealed for 4 minutes. The annealing was done in a nitrogen surrounding [8].

2.4 Organic Solar Cells with Nanocrystals

The use of inorganic nanocrystals in solar cells has several advantages including: controlled synthesis, solution processability and a decreased sensitivity for substitutional doping, while retaining the broadband absorption and superior transport properties of the traditional inorganic semiconductors. The nanocrystals have another advantage, namely, the nanocrystal's bandgap is tunable. By controlling the size of the nanocrystals during synthesis, the band gap can be tuned thanks to the quantum confinement.
In order to overcome the low electron mobility of organic materials, solar cells were produced using nanocrystals in combination with hole conducting polymers. Efficiencies where reported up to ~2% under AM 1,5 conditions using CdSe nanorodd and P3HT [9].

Additionally, solar cells consisting of only inorganic nanocrystals were produced. The active layer consists of a blend of two types of nanocrystals (or nanorods) that provides the D/A couple. Solar cells made with CdTe and CdSe nanocrystals have efficiencies of almost 3% [10].

Another alternative way to increase the efficiency of solar cells is using a three component blend. The idea is based on the ´traditional´ donor/acceptor couple with an additional third component; the nanocrystals. The nanocrystals could offer more excitons by absorption in the near infrared and thereby the number of excitons increases. To create such a situation it is necessary that the HOMO of the hole transporter has a higher energy compared to the conduction band of the nanocrystal and, in the same way, the LUMO of the electron transporter has an energy which is lower compared to the valence band energy of the nanocrystal. This is depicted in figure 3 [11].

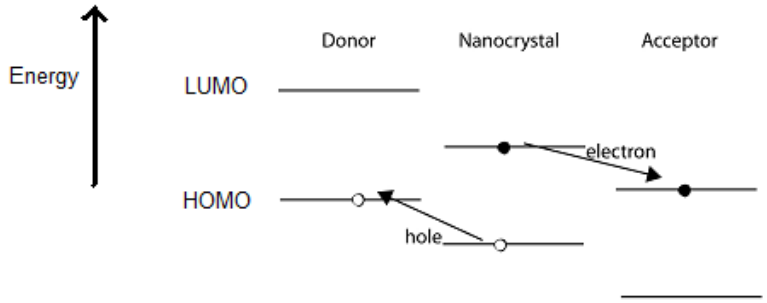

Fig. 3: The optimal energy band allignment for a 3 component blend for solar cell application.

In this situation the holes that are created will be transferred to the hole transporter, which is the donor, by energy considerations. The hole wants to be in the higher energy band. For the electron it is exactly the opposite, the electrons want to be in the energetic most favoured band, which is the lowest energy band. When such a photoactive layer is made the energy conversion efficiency should be increased thanks to the new absorption band due to the presence of the nanocrystals in the active layer. Because of the tunability of the nanocrystals the solar cells can be made sensitive in the region of interest, i.e. in the infrared region.

In figure 3 the process within the two component blend, in which the electrons and holes between the donor and acceptor are exchanged, is not shown. Only the behaviour of the excitons, created in the nanocrystals, is shown.

3 Experimental Details

In this chapter the experimental details will be discussed. In the first paragraph the different materials, which are used in the production of the solar cells, will be described. After the materials, the production process will be described in detail followed by the measurement procedure.

3.1 Materials

The solar cell consists of, as mentioned before, a photoactive layer sandwiched between two electrodes, all on a glass substrate. The different materials which are used for the experiment are denoted and discussed in this section.

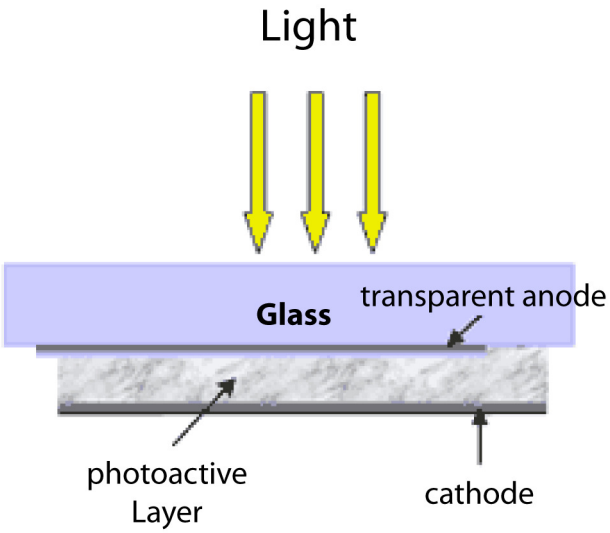

Fig.4: Schematic picture of standard solar cell.

3.1.1 Glass and indium tin oxide

For the processing of the cell a square shaped glass substrate with an indium tin oxide (ITO) layer is used. The size of the substrate is 3 x 3 cm. At this substrate 4 rectangular areas of ITO – of different sizes – are deposited. ITO is transparent in thin layers and is conducting. It is a solid solution of Indium(III)oxide (In_2O_3) and tin(IV)oxide (SnO_2) and it is an n-type semiconductor with a high work function of approximately 4,8 eV [12]. Due to this high work function it is an excellent material to serve as hole injecting or extracting electrode.

3.1.2 PEDOT:PSS

On top of the ITO a PEDOT:PSS layer is applied. PEDOT is poly(3,4-ethylenedioxythiophene) which is a transparent conducting polymer. PSS is polystyrenesulfonic acid which is a polymer based on polystyrene. A water-based blend of these two materials is spin-coated on the substrates. Its reduces the hole injection barrier at the interface of the ITO contact by its workfunction. The work function of the PEDOT:PSS is 5,2 eV [13]. The material is also very suitable for charge carrier transport because of its low resistivity.

3.1.3 Poly(3-hexylthiophene)(P3HT)

On top of the PEDOT:PSS layer, the photoactive layer is processed. As mentioned in the theory section, the photoactive layer consists of several materials of which one could be P3HT. In our photoactive layer regio-regular P3HT was used.

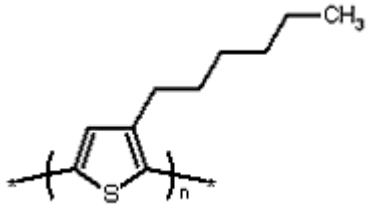

Fig. 3-2: the chemical structure of RR P3HT

P3HT is shown in fig. 3-2, the polymer is regio-regular which means that the coupling between the monomers is the same through the polymer with a constant position of the alkyl chain respect to the thiophene unit. By using regio-regular P3HT instead of regio random P3HT, the layer is more crystalline. The higher crystallinity turns out in higher charge mobility and better solar cell performances. The HOMO and the LUMO of P3HT are at –4,9 eV and –3,0 eV [11].

3.1.4 PCBM

PCBM is a C_{60} derivative and is mixed with P3HT or P3HT/PbS in the photoactive layer.
PCBM is [6,6]-phenyl C_{61} butyric acid methyl ester as shown in figure 3-3. The C_{60} is functionalized because C_{60} is not soluble and therefore hard to process. The HOMO and LUMO level of PCBM are –6,1 eV and –4,3 eV [11].

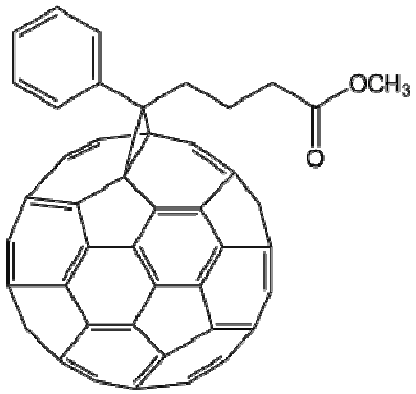

Fig.5: chemical structure of the PCBM molecule

3.1.5 PbS nanocrystals

There is a third material introduced in the blend, the nanocrystals. The nanocrystals that are used are lead sulfide (PbS) nanocrystals. The nanocrystals are synthesized in colloidal form by capping with a molecular-ligand shell, determining their solubility and limiting their charge-transport properties. The valence band energy of the used nanocrystals is –5,25 eV and the conduction band energy is –4,28 eV. So the bandgap is positioned, in respect with the energy levels of P3HT and PCBM, in such a way which was shown and described in section 2.4. [11]

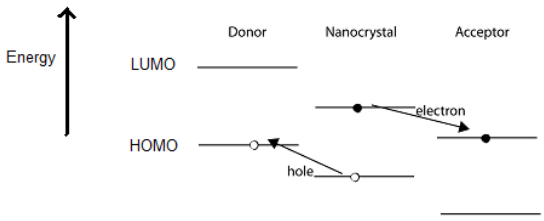

Fig. 3: The optimal energy band allignment for a 3 component blend for solar cell application.

3.1.6 Aluminium and Lithium Fluoride

To complete the device we need to evaporate a top contact. The top contact consists of a small (usually 1 nm) lithium fluoride layer on top of which is evaporated an aluminium layer of 100-200 nm thickness. Lithium fluoride has a low work function compared to aluminum, so when a lithium fluoride layer is added the total work function is lowered, resulted in improved electrode properties. The lithium fluoride increases the performances of the solar cell of about 20% [14].

3.1.7 Solvents

In the fabrication process different solvents are used.

Chlorobenzene
Chlorobenzene (CB) is a benzene derivative whith an additional chlorine group. It is colourless and highly flammable. It is a very good solvent for organic compounds, but highly toxic. It has a boiling point of 131 °C [15].

Ortho-dichlorobenzene
Ortho-dichlorobenzene (ODCB) is a benzene derivative as well as chlorobenzene, but housing two additional chlorine groups. In ODCB the two chlorine groups are positioned next to each other. The boiling point of ODCB is 179 °C which makes it a very useful solvent in slow drying processes. Like CB, ODCB is colourless, harmful and very flammable [16].

Chloroform
Chloroform (CF) is also colourless, like ODCB and CB, and an ultimate solvent for polymers. It has a low boiling point (61,2 °C) which makes it very volatile. Because of this the fabrication is a fast drying process [17].

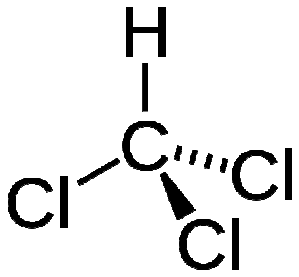

Fig. 4: A schematic representation of the chloroform molecule

3.2 The device manufacturing process

The device fabrication is done in a cleanroom environment and most of the processing was done in inert atmosphere.

3.2.1 The solution

The first step in de manufacturing process is the preparation of the solution. In the solution the donor-acceptor couple are mixed in a solvent. The mass ratio between the donor:acceptor is 1:1. Concentrations are usually around ~10–20 mg/ml. After the solvent is added, the bottle is sealed with parafilm and left overnight while stirring, using stirring magnets and a magnetic plate, in a glovebox at room temperature. When needed, the solution is put on a hotplate (usually at a temperature of 70 °C), which is also magnetic, so the solution is stirred and heated over night. Before processing the active layers, the nanocrystals are added to the solutions in different concentrations and left stirring for at least half an hour.

3.2.2 The cleaning process

After the solution is made, the next step is the proper cleaning of the ITO substrates. The cleaning takes place in a wet-station. The first cleaning step is scrubbing the substrates with a soap:demi-water (1:10) solution which had a temperature of at least 70 °C. Each ITO substrate has to be scrubbed for 5 minutes, using the soap solution and plastic scrubbing gloves. This removes spikes and dirt from the ITO surface. After the scrubbing all the substrates are put in a flow bath of demi-water for at least 5 minutes. When this is done the substrates are put in acetone and placed in an ultrasonic bath for another 5 minutes. Then the substrates are put back in the demi-water flow bath for 5 minutes again. Afterwards, the substrates are put in isopropanol and placed in an ultrasonic bath for another 5 minutes. To dry the substrates, after the cleaning, a dry spinning machine and a oven (at 140 °C) is used at which the samples are left for at least 10 minutes. After the oven, the substrates are put in the UV-ozone cleaner for 20 minutes in order to remove the remaining organic parts.

3.2.3 The PEDOT:PSS spin coating

When the cleaning process is finished the PEDOT:PSS layer is spin-coated at the substrates. The spin-coating program which is used consists of two steps. The first step is using a rotational speed of 500 rpm for 10 seconds to spread around the PEDOT:PSS solution on the substrate. The second step is using a rotational

speed of 1500 rpm for 50 seconds to obtain a layer thickness of around 50 nm. The spin-coating is done in air. Prior to the spin coating the PEDOT:PSS solution is shaked and filtered. After the spin-coating the substrates are put back in the oven for another 10 minutes at 140 °C, to remove the water from the PEDOT:PSS solution. Afterwards the substrates are put in a container and transported to a nitrogen filled glovebox in order to deposit the active layer on top of the substrates.

3.2.4 Spin-coating

One of the methods which is generally used to put the photoactive layer is the spin-coating. Before the solution needs to be filtered in order to remove aggregates and dust particles. The photoactive layer is spin-cast using a Karl Suss spin-coater. The layer thickness can be varied by the concentration of materials, different solvents and the spin-coating program. The spin-coater is equipped with a lid which can be opened and closed, as edit in the spin-coater program.

3.2.5 Doctor-blading

Another way to put the photoactive layer, on the substrates, is the doctor blading method. In accordance to the spin-coating method, the solution needs to be filtered before use. Doctor blading is a method which is also called tape casting or knife coating and it is based on a large hot plate which temperature can be controlled. On this we put the substrate with ITO and PEDOT:PSS and a glass substrate with the same size is put next to each other on the plate. The solution is put at the edge of the glass substrate and spread over the substrate by a blade which is moving over the substrate with a constant speed. Parameters which have to be considered in this process are the evaporation rate, the viscosity of solvent, the process velocity, the contact angle between the solution and the substrate, the temperature of the plate and the height of the blade above the substrate.
In this research the temperature, the blading speed and the height of the blade are varied.

3.2.6 Annealing

After the active layers are processed on the substrates the samples are annealed. Most of the samples were annealed at 110 °C for 5 minutes.

3.2.7 Evaporation of the top electrodes

To finish the device top electrode needs to be evaporated. First a lithium fluoride layer of 1 nm thickness evaporated followed by a 100 nm aluminium layer. The samples are put in the evaporation chamber which is slowly rotating. The LiF and Al are placed in two different boats which a current can run through. The system is pumped down to a pressure below 10^{-6} mbar. After the system is pumped down to the proper pressure a current is applied which runs through the boats. In this way the boat is heated and the material for the top contact can be evaporated. Both the lithium fluoride and the aluminium layer can be evaporated using a pre-programmed deposition method. Due to the evaporation masks there are four areas where the materials are evaporated and partially overlap with the ITO electrodes. This way there are 4 areas obtained which represent our four solar cells. The sizes of the four areas are 9, 16, 36 and 100 mm^2.

3.2.8 Spin-coating programs

The different programs that are used are the following:

The different spin-coating programs which are used for chlorobenzene based solutions:

Speed 300 rpm, acceleration 300 rpm/s, time 120 sec with lid closed (1.1)

Speed 500 rpm, acceleration 500 rpm/s, time 120 sec with lid closed (1.2)

Speed 800 rpm, acceleration 800 rpm/s, time 120 sec with lid closed (1.3)

Speed 1000 rpm, acceleration 800 rpm/s, time 120 sec with lid closed (1.4)

Speed 1200 rpm, acceleration 1000 rpm/s, time 120 sec with lid closed (1.5)

Speed 1500 rpm, acceleration 1000 rpm/s, time 120 sec with lid closed (1.6)

Spin-coating programs for chloroform based solutions:

Speed 500 rpm, acceleration 500 rpm/s, time 3 sec with lid closed, then
Speed 1000 rpm, acceleration 1000 rpm/s, time 60 sec with lid closed, then
Speed 1000 rpm, acceleration 1000 rpm/s, time 30 sec with lid open (2)

Spin-coating programs for orthodichlorobenzene based solutions:

Speed 1000 rpm, acceleration 1000 rpm/s, time 120 sec with lid closed (3)

3.2.9 Doctor Blading parameters

As described in section 3.2.5 there are several parameters which are varied when the active layer is doctor bladed. The varied parameters are listed below.

Temperature is varied between 60 - 80 °C.
The blading speed is varied between 25 - 35 mm/s.
The blade height is varied between 8,5 - 9,5 mm.

The height denoted is the height of the blade in respect with the plate on which the samples are put.

3.3 Characterisation

3.3.1 J-V characteristics

The completed device can be characterized by J-V measurements. This is done in a nitrogen filled glovebox outside the cleanroom. The devices are transported to the glovebox in a nitrogen filled container. The measurement setup consists of a sample holder which has eight contact points, two for each area. One of these is in contact with the cathode and one with the anode. Since the active layer covers ITO contacts it needs to be removed by scratching because otherwise there is no efficient contact with the ITO electrodes. When the sample is put in the holder correctly, a DC current can be applied across the device. The J-V measurements are done with a Keithly 2400 source meter. The data is collected and recorded using a computer with National Instruments LabVIEW software. The light source used is a white light metal halide lamp. The light source needs to be calibrated before measurements are done, using a silicon diode. When the calibration is done, the devices are illuminated with an intensity of 1000 W/m^2, which is equal to one sun intensity. From the data, the characteristics of the solar cell can be found. The V_{OC}, I_{SC}, FF and the η can be calculated. During the measurements the temperature is measured and can be considered at constant room temperature of 295 K.

3.3.2 Layer Thickness

After the J-V characteristics are measured the layer thickness is also determined. This is done in air using a Dektak 6M profilometer in the cleanroom. The devices are transported in a container which is still under nitrogen. Using a tweezer a scratch is made in the photoactive layer. Then a profile scan is made, in the transverse direction, across the scratch. When measuring the difference in surface height between a point in and a point out of the scratch, the layer thickness is obtained. From the profile scan the thickness of the active layer can be determined by measuring the difference between the depth of the scratch and the height of the active layer.

3.3.3 AFM images

AFM images of a few selected devices are performed. AFM stands for Atomic Force Microscopy and is a very high-resolution type of scanning probe microscope. The images offer extra information about the surface morphology of the devices which helps to understand or further improve the device performance.

4 Experimental results and discussion

In this chapter the results are shown and discussed. First the doctor blading devices are discussed. The processing, the device performances and the thickness of the layers are considered. After the doctor blading the spin-coating of the different layers, based on different solvents is discussed. The device performances are shown and explained. In addition some AFM images are also shown and discussed.

4.1 Solar cells prepared by doctor blading

As described in chapter 3 there are different methods which can be used to process the photoactive layer in the device. One of the promising methods is doctor blading. On of the benefits of doctor blading is that it requires a relatively low amount of material compared to spin-coating. The donor/acceptor couple which is used as reference is the P3HT/PCBM couple and nanocrystals are added prior to the processing to this blend in order to see the effect of the nanocrystals and increase the efficiency of the devices.

The weight ratio between the P3HT:PCBM was 1:1. When the nanocrystals are blended with the P3HT/PCBM the weight ratio PbS:P3HT:PCBM is varied. Because the nanocrystals are already provided in solution there has to be taken account of the concentration of the different solutions to obtain the desired weight ratio. The concentration PCBM/P3HT, solved in chlorobenzene, is varied between 10-20 mg/ml but 20 mg/ml turned out to be optimal.
When the desired ratios are obtained, the solution can be doctor bladed on the substrates on top of ITO and PEDOT:PSS.

At first the influence of changing the different parameters on the layer thickness is studied, by doctor blading a PCBM/P3HT solution without nanocrystals. The parameters that are changed are the temperature and the blading speed. The obtained layer thickness's for the different parameters are shown in diagram 4-1.

Temperature (°C)	Speed (mm/s)	Layer Thickness (nm)
60	25	90
70	25	120
	30	145
	35	128
80	25	80
	30	114
	35	120

Table 1: The layer thickness obtained when manufacturing a P3HT/PCBM layer on glass substrate for different temperatures and speed.

One can see in table 1 that the layer thickness is difficult to control. When the speed is increased at a temperature of 70 °C, first the layer thickness is increasing while at a higher speed the layer thickness is decreasing. The main conclusion that can be drawn is that the layer is getting thicker when the blading speed is increased, however it cannot be shown consistently in every case.

When PbS nanocrystals are added to P3HT/PCBM solution and processed on glass substrate, two temperatures (60 °C and 70 °C) and a blading speed of 25 mm/s are used. These parameters are chosen because the layer thickness was optimal for the P3HT/PCBM blend at these parameters.

Temperature (°C)	Speed (mm/s)	Layer Thickness (nm)
60	25	80
70	25	85

Table 1: The layer thickness obtained when manufacturing an P3HT/PCBM/PbS layer on glass substrate for different temperatures at constant speed.

Out of the temperature variation there can be seen that a temperature of 60 °C and 70 °C are desirable, above 80 °C the solvent evaporated too fast and a inhomogeneous layer is obtained.

Layers with a thickness of 100-150 nm are considered to be the optimum. Therefore samples are processed on ITO substrate, with a blading speed of 25 mm/s and at a temperature of 70 °C. The height of the blade is varied as well. Reference P3HT/PCBM devices and P3HT/PCBM/PbS are produced to investigate the effect of PbS nanocrystals in the blend.

Blend	Height of the blade (mm)	Efficiency (%)	Layer Thickness (nm)
P3HT/PCBM/PbS	8,5	0,19	150-160
	9,0	0,26	160-200
	9,5	0,25	250-290
P3HT/PCBM	8,5	0,93	370-380
	9,0	1,06	325-335
	9,5	1,26	270-280

Table 2: Parameters of P3HT/PCBM and P3HT/PCBM/PbS solar cells when the height of the blade is varied with doctor blading. Measurements where done at a temperature of 70 °C and at a blading speed of 25 mm/s.

It can be concluded that for all the produced samples the reference devices show significantly higher efficiencies compared to the three component cells. The thickness of the layers are determined and the reference sample has generally flat surface and homogeneous layer while the three component layers exhibit very rough surfaces with inhomogenities. Moreover, by adding nanocrystals in the P3HT/PCBM solution the wettability of the substrate changes, probably due to the effect of the ligands around the nanocrystals.
The highest efficiency is obtained at a blade height of 9,0 mm. This processing method is repeated and then the blading speed is decreased to 20 mm/s.

Blend	Blading Speed (mm/s)	Efficiency (%)	Layer Thickness (nm)
P3HT/PCBM/PbS	20	0,38	160-200
	25	0,55	200-300
P3HT/PCBM	25	0,46	400-450

Table 3: The results of producing solar cells by doctor blading, varying the speed of the blade. For both a "traditional" P3HT/PCBM cell and the "new" three component P3HT/PCBM/PbS cell. Measurements where done at a temperature of 70 °C and at a blading height of 9,0 mm.

The three component system show slightly higher efficiencies in comparison with the reference system. The difference in efficiency is ~0,1%. The efficiency of the three components is more than doubled and the reference efficiency is decreased of a factor two. Even though the devices made with the three components blend has a higher efficiency compared with the reference device, the efficiency is still very low, compared to the optimized P3HT/PCBM devices, which can reach efficiencies up to 5%. However, the reproducibility of the devices is challenging.

In conclusion the main problem with the doctor blading is the reproducibility. As it was already shown, the devices can perform totally different, even when they are

processed under the same conditions. Furthermore the layers, when the nanocrystals are added, become very rough.
Nice and flat layers are desired to achieve an optimal cathode deposition, an elevate roughness can cause penetration of the metal in the layer and consequently electrical shorts.

4.2 Solar cells prepared by spin-coating

Besides doctor blading, which did not give very high efficiencies, spin-coating of the active layer is another way to build devices. The spin-coating program was varied in order to optimize the layer and thereby increase the efficiency of the devices.

The weight ratio in the blend, used for the spin-coating, are approximately the same as used for the doctor blading: P3HT:PCBM:PbS is 1:1:1. The total concentrations of the solutions was varied in the range of ~5-20 mg/mL (usually 15 mg/mL).

The first spin-coating program used was program 1.2 as described in section 3.2.8. The results are shown below in table 4-5.

Blend	Efficiency (%)	Layer Thickness (nm)
P3HT/PCBM/PbS	0,42	190-210
P3HT/PCBM	1,07	250-260

Table 5: Efficiency and layer thickness, of both the three component and the reference device. Layers are spin-coated by program 1.2. Temperature is 295 K.

The difference between the three component blend and the reference is significant, the reference device shows better performance which was observed in the case of doctor blading.

In order to optimize the device, four different spin-coating programs are tried, program 1.1 – 1.4. The results are shown in table 4-6.

Blend	Spin coating program	Efficiency (%)
P3HT/PCBM/PbS	1.1	0,07
	1.2	0,09
	1.3	0,22
	1.4	2,07
P3HT/PCBM	1.1	1,66
	1.2	2,36
	1.3	0,14
	1.4	1,99

Table 6: The efficiencies of the three component device and the reference device obtained using different spin-coating programs. Temperature is 295 K.

We see a higher efficiency for the three component device compared to the reference when program 1.4 is used. The I-V characteristics of the devices, using different spin-coating programs, are shown.

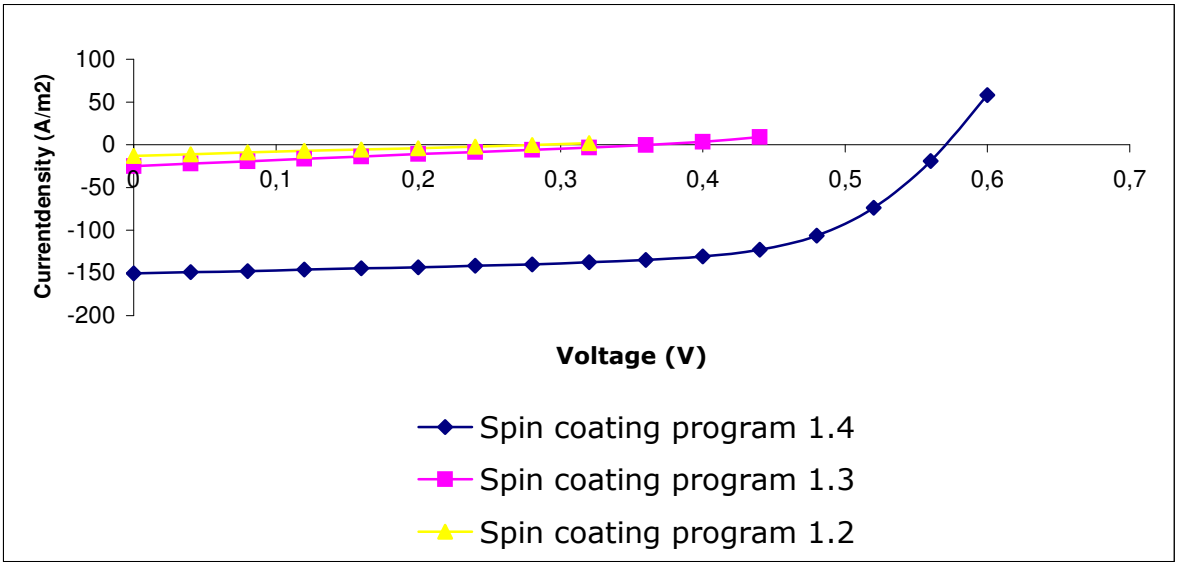

Fig. 6: J-V characteristics of P3HT/PCBM/PbS devices using different spin coating-programs.

In the figure we see that when the spin-coater speed is increased in the program – spin-coating program 1.4 is the fastest – the shape of the curve is improved and both the V_{OC} and the J_{SC} are increasing, leading to better performances. The fact that the efficiency of the three component device is higher compared to the reference is very promising, implying that the PbS nanocrystals are absorbing causing an increase of the device efficiency.

AFM images of the three devices, of which the I-V characteristics are displayed in figure 7, were measured. These are shown below in figures 8 and 9.

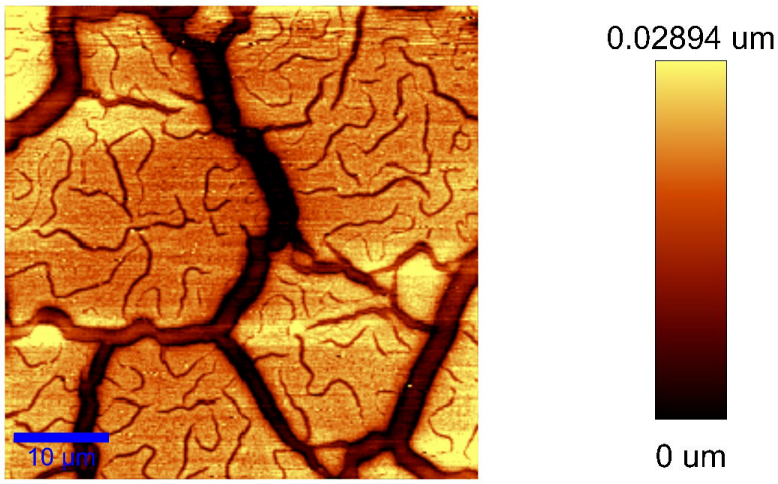

Fig. 7: AFM image of the P3HT/PCBM/PbS device processed by using spin-coating program 1.2

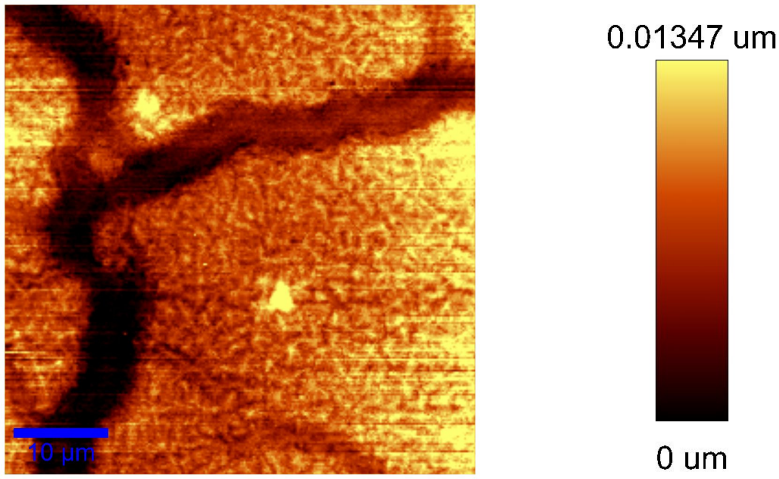

Fig. 8: AFM image of the P3HT/PCBM/PbS device processed by using spin-coating program 1.3

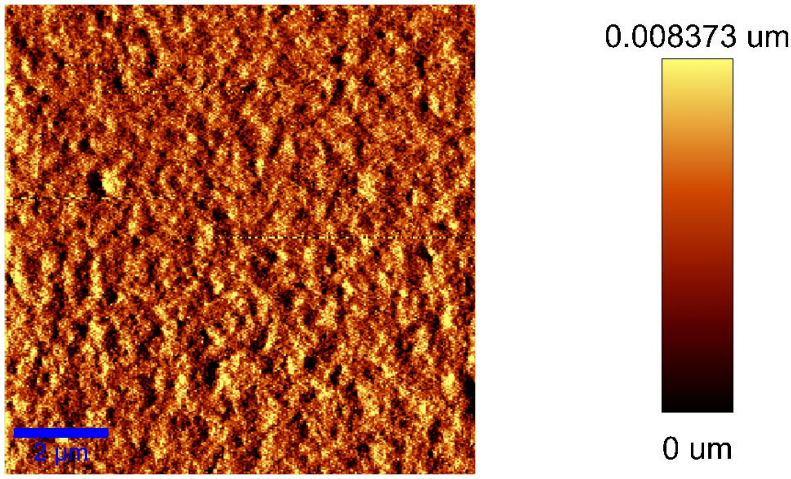

Fig. 9: AFM image of the P3HT/PCBM/PbS device processed by using spin-coating program 1.4

The AFM images explain why the efficiency of devices obtained with spin-coating program 1.4 is higher than the one fabricated with program 1.3 and 1.2. In the first two images the layers are not homogenous; there are some channels, which strongly decrease the efficiency of the device. The AFM image in figure 9 shows a very nice and smooth layer. In this case the exciton can be transported efficiently to the interface at which charge separation can occur, which was confirmed by device performances next to AFM.

However, the problem of reproducibility remains, most probably due to morphology issues, namely the nanocrystrals have a strong influence on the wetting and the morphology. Moreover, the spin-coating spin is further increased since better performances are obtained when the active layer was spin-coated by a faster program.

Blend	Spin coating program	Efficiency (%)
P3HT/PCBM/PbS	1.4	0,12
	1.5	0,10
	1.6	0,07
P3HT/PCBM	1.4	0,71
	1.5	0,95
	1.6	1,43

Table 4: for each different spin-coating program the efficiencies are presented, as well for the three component device as the reference. Temperature is 295 K.

The efficiencies of the three component devices did not increase further but lowered. The efficiencies of two devices, which are processed in the same way, are totally different and could differ around a factor 20. In addition the reference devices show higher efficiencies than the three component device.

There had also been an attempt to replace the chlorobenzene by chloroform to investigate the influence of the solvent. The concentration of the P3HT and PCBM in chloroform is 10 mg/mL and the active layer is spin-coated by program 2. Results are shown in table 8.

Blend	Spin coating program	Efficiency (%)
P3HT/PCBM/PbS	2	0,06
P3HT/PCBM	2	1,78

Table 5: P3HT/PCBM/PbS and reference device efficiencies when processed from chloroform.

The efficiency of the three component device is very low compared to the reference. Device efficiencies could not be increased further, even when the solvent is changed.

5 Conclusions

As final conclusion the idea of a three component device is promising since few of the fabricated devices showed higher efficiencies than the P3HT/PCBM reference solar cell. In these cases the PbS nanocrystals seem to be active and induce an increase in efficiency up to 2,07%. Hopefully, a further optimization and control of the morphology will in future solve the problem of reproducibility and the efficiencies can be further improved.

The effect of increasing speed of the spin-coater, at the layer morphology is clearly demostrated. When the spin-coating speed is increased from 500 rpm to 1000 rpm, the layer becomes smoother. Big clusters and channels, which are seen in AFM images of the lower speed processed layers, disappear when the spin-coating speed is increased. Optimal device performances are obtained when the active layer is spin-coated with 1000 rpm, 800 rpm/s for 120 seconds.

The main problem in both doctor blading and spincoating is the reproducibility. Both in spin-coating and in doctor blading there are very different results obtained for devices which are processed under the same conditions. Clearly small changes in experimental conditions have huge influence on the device performances. Especially the blends containing PbS nanocrystals are difficult to process due to changes in wettability of the substrates.

The best results are obtained by using chlorobenzene. When the solvent is changed into chloroform a small decrease in cell performances is noticed contrary to the reference device which showed higher efficiency.

Acknowledgements

I want to thank dr. Maria Antonietta Loi for giving me the opportunity to do my bachelor project in her research group and giving me the guidance when I needed. My gratitude goes to my supervisor Krisztina Szendrei, who explained me the theory, taught me how to work in the cleanroom and helped me when I needed help. I want to show my appreciation to the technical staff, Jan Harkema and Frans van der Horst, for helping me around when I needed technical assistance. Also I would like to thank Oleksandr, Dorota, Herman, Martijn, Auke, Johan, Paul and Ilias for helping and guiding me. I would also like to thank all the other members of the group.

References

[1] M. A. Green1, K. Emery, Y. Hishikawa and W. Warta, *Progress in Photovoltaics* **17** (2009), 321

[2] L. M. Popescu, *Fullerene based Organic Solar Cells*, (drukkerij van Denderen BV., Groningen, The Netherlands, 2008)

[3] P. W. M. Blom, V. D. Mihailetchi, L. J. A. Koster, D. E. Markov, *Adv. Materials* **19** (2007), 1551

[4] C. J. Brabec, N. S. Sariciftci, J. C. Hummelen, *Adv. Funct. Materials* **19** (2001) 15

[5] J. J. M. Halls, J. Cornill, D.A. dos Santos, R. Silbey, D.H. Hwang, A. B. Holmes, J. L. Brébas, R. H. Friend, *Phys. Review B* **60** (1999), 5721

[6] C. W. Tang, *Appl. Phys. Letters* **48** (1986), 183

[7] S. Gűnes, H. Neugebauer, N. S. Sariciftci, *Chem. Review* **107** (2007), 1324

[8] V. D. Mihailetchi, H. Xie, B. de Boer, L. J. A. Koster, P. W. M. Blom, *Adv. Funct. Materials* **16** (2006) 699

[9] W. U. Huynh, J. J. Dittmer, A. P. Alivisatos, *Science* **295** (2002) 2425

[10] I. Gur, N. A. Fromer, M. L. Geier, A. P. Alivisatos, *Science* **310** (2005) 462

[11] T. Rauch, M. Boberl, S. F. Tedde, J. Fust, M. V. Kovalenko, G. Hesser, U. Lemmer, W. Heiss and O. Hayden, *Nature Photonics* **3** (2009) 332

[12] V. Bliznyuk, B. Ruhstaller, P. J. Brock, U. Scherf, S. A. Carter, *Adv. Materials* **11** (1999) 1257

[13] F. Zhang, M. Johansson, M. R. Andersson, J. C. Hummelen, O. Inganas, *Adv. Materials* **14** (2002) 662

[14] C. J. Brabec, S. E. Shaheen, C. Winder, N. S. Sariciftci, *Appl. Phys. Lett.* **80** (2002) 1288

[15] Wikipedia, the free encyclopedia, Chlorobenzene

[16] Wikipedia, the free encyclopedia, Chloroform

[17] K. Szendrei et al. *Adv. Materials* **21** (2009), 683

[18] Vishal Shrotriya et al. *Chemical physics letter* **411** (2005) 138[19] Oleksandr V. Mikhnenko et al. *Journal of physical chemistry* **113** (2009) 9104